Journal of the European Ceramic Society 20 (2000) 169–176

Microstructure development and densification of ultrafine Y-TZP monoliths obtained by seeding-assisted chemical coprecipitation

J. Tartaj [a,*], E. Lachowski [b], J.F. Fernández [a], C. Moure [a], P. Durán [a]

[a] *Electroceramics Department, Instituto de Cerámica y Vidrio (CSIC), 28500-Arganda del Rey, Madrid, Spain*
[b] *University of Aberdeen, Department of Chemistry, Scotland, UK*

Received 15 February 1999; received in revised form 23 April 1999; accepted 11 May 1999

Abstract

Y-TZP seeded gel monoliths have been prepared by a sol–gel method based on the coprecipitation of Zr^{4+} and Y^{3+} precursors as hydroxides and the stabilisation of the suspension in pure ethanol with a disc turbine. The addition of solid Y-TZP nanometer-size seed particles (10 wt%) into the Y-TZP precursor solution plays a crucial role during crystallisation and densification of monoliths. Basically, it induced a preferential nucleation, which enhanced the crystallisation kinetics and the activation energy is fairly lowered As a result of the increased nucleation frequency for the crystallisation process a well-developed homogeneous porous microstructure is obtained facilitating the sintering and so the densification at lower temperatures. In this way, Y-TZP highly densified ceramic monoliths have been obtained at 1050°C, with a grain size within the nanometer range.

Keywords: Sol–gel processes; ZrO_2–Y_2O_3; Seeding; Sintering

1. Introduction

In the last few years increasing efforts are being directed towards synthesis of nanocrystalline powders. Consolidation of loosely agglomerated nanoparticles (less than 10 nm) of ceramic materials is expected to result in significant payoffs. For example, by consolidation of nanoparticles, the sintering temperature can be lowered by several hundred degrees and thus, avoid the use of sintering aids. Problems such as decomposition of constituent phases that are frequently found in the sintering of nitrides, and deleterious interfacial interactions can be solved by using nanoparticles as the starting raw materials. Moreover, smaller grain sizes should result in improved mechanical properties and superplastic behaviour for net shape forming. Nanocrystalline powders have been produced by several techniques.[1–5] Among them hydrothermal synthesis is an attractive method for the preparation of nanocrystalline powders. The process which involves precipitation from aqueous solutions under conditions of high temperature (200°C–300°C) and pressure (20–30 bar), has been widely used for the synthesis of the very fine powders. Recently, the inert gas condensation technique has received great interest for the synthesis of nanocrystalline powders. Some problems of agglomeration during the oxidation step (at ~300°C), in this technique, limit the quality of the obtained powders. Other techniques such as vapour deposition methods, spray and flame pyrolysis, laser-ablation, etc, also lead to powders in the nanometer range. Difficulties in most of them, mainly in the cost and control of the composition, precludes their utilisation. The sol–gel from aqueous and/or alcoholic solutions seems to be the promising route for making nanocrystalline Y-TZP powders. In multicomponent gels the greatest degree of homogeneity is achieved by polymerisation of double alkoxides or dissolving two alkoxides in a mutual solvent, the problem is that not all double alkoxides are available and not all combinations of alkoxides lead to complex formation, then the relative rates of hydrolysis and condensation of the alkoxides will determine the degree of chemical homogeneity of the resulting gel. For these reasons, alternative routes such as sol-precipitation of inorganic salts with the formation of a colloidal gel and the use of precursors formed through the reaction of the alkoxide with an organic or inorganic salt can be utilised.

For the production of dense consolidated bodies for superplastic forming operations on a commercial scale, two main requirements must be fulfilled, (i) the availability of non-agglomerated (or very soft primary crystallite

* Corresponding author.

0955-2219/00/$ - see front matter
PII: S0955-2219(99)00144-2

clusters) nanocrystalline powders in reasonable amounts and (ii) the nanocrystalline powders must have a high flowability leading to the achievement of defect-free compacted green bodies.

Albeit the sol-precipitation method could be adequate to produce massively nanocrystalline powders, the relatively high calcination temperature used (500–600°C), gives rise to the formation of reasonably high interparticle bonds, which detrimentally influence both sinterability and the compactability of the calcined powders. In this way, it has been establish in previous work[6,7] that the crystallisation temperature is the key parameter controlling the strength of the interparticle bonds, i.e. the lower the crystallisation temperature, the lower the strength of the interparticle bonds. Applying the "seeding fundamental concepts"[8,9] to the Y-TZP system, a well–crystallised yttria-doped tetragonal zirconia powder can be obtained at a temperature as low as 375°C. Such a powder, after compacting, led to almost fully dense bodies with grain size within the nanometer-scale on sintering at 1050°C.[10]

The aim of the present work is the preparation of seeded Y-TZP monoliths by a sol-precipitation method based on the coprecipitation of Zr^{4+} and Y^{3+} precursors as hydroxides and the stabilisation of the suspension in alcohol and, to study their direct sintering behaviour. The approach adopted involved the incorporation of solid Y-TZP nanometer-size seed particles into the Y-TZP amorphous matrix. A commercial (Tosoh) Y-TZP powder will be taken as a reference.

2. Experimental procedure

Y-TZP (3 mol% Y_2O_3) precursors have been prepared by dissolving in adequate proportions $ZrOCl_2$ and $YCl_3.6H_2O$ in a mixture of water/isopropanol. For seeded samples, at this point, crystalline Y-TZP seed particles prepared as described elsewhere,[10] within a nanometric range (≈6 nm), as determined from the analysis of X-ray fine broadening using the Sherrer formula,[11] were suspended in pure isopropanol, and added

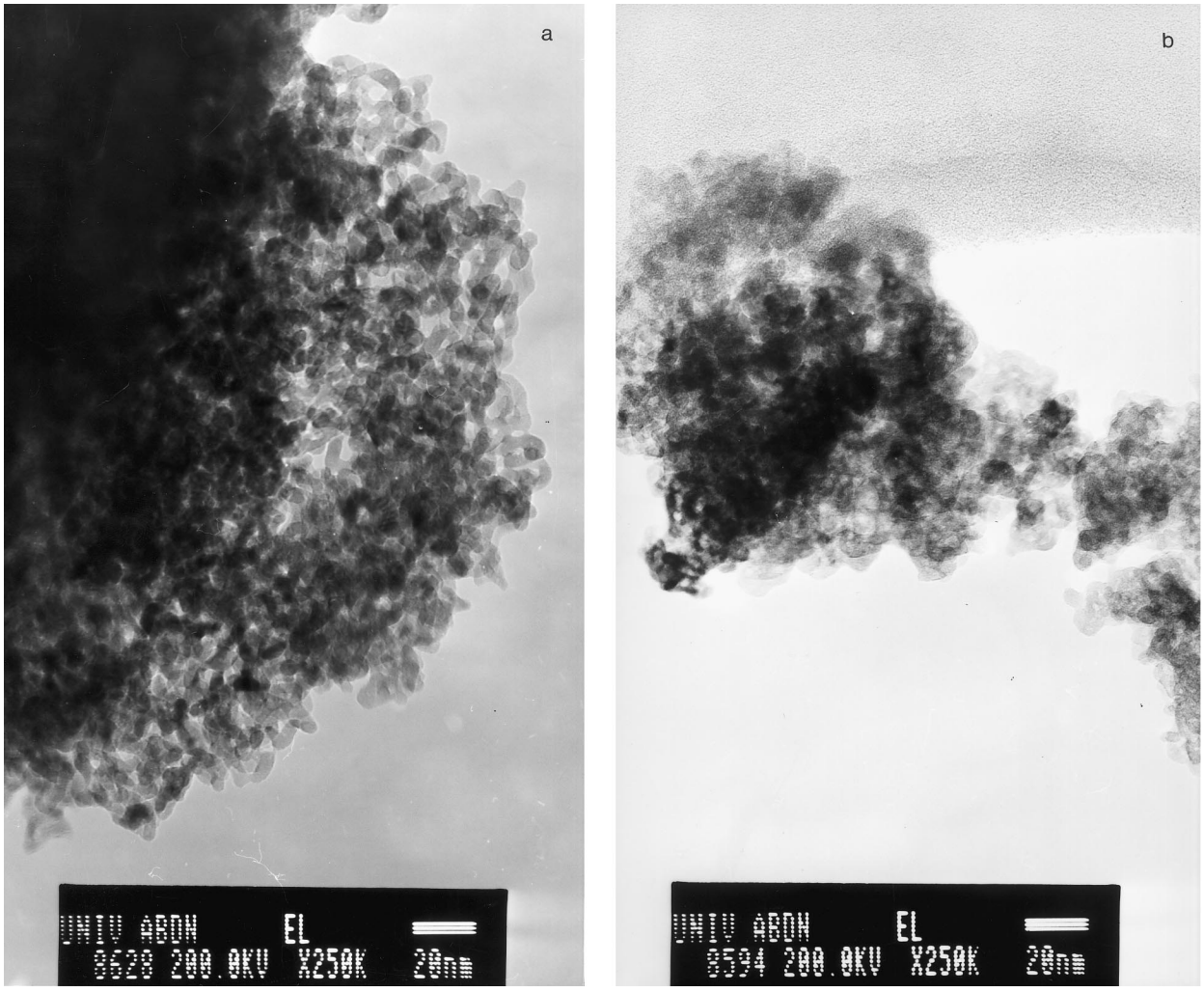

Fig. 1. TEM micrographs of Y-TZP powders calcined at 350°C, (a) 10 wt% seeded and (b) unseeded.

to the transparent Y-TZP solution to obtain 10 wt% seeded Y-TZP monoliths (3×10^{16} seeds/g of gel crystallised). The final ratio of water/isopropanol was 1/1 in volume. To ensure a homogeneous dispersion of the Y-TZP seeds in the Y-TZP precursors solution, a powerful agitation was maintained for 60 min. A mixture of isopropanol $+NH_4OH$ 1/1 in volume was added to the precursor solution containing the seeds in suspension up to complete coprecipitation of the Zr^{4+} and Y^{3+} hydroxides (pH≈8–9). A continuous stirring was maintained during and after the precipitation process, avoiding the agglomeration and deposition of the seeds at the bottom of the beaker and, therefore, the seed particles were homogeneously widespread through the precipitate.

The amorphous gelatinous precipitates, unseeded and 10 wt% Y-TZP seeded, were washed with butylamine in the first place to eliminate residual chlorides; distilled water for the removal of the anions of the salt solution used, as the anions may help the formation of salt crystals joining individual particles and cause the formation of hard agglomerates; and pure ethanol to avoid the presence of water. A thorough washing step with alcohol, with a lower surface tension than that of water, play a crucial role in reducing the capillary force and producing soft agglomerates.[12] After this, the precipitates were dispersed in pure ethanol with a disc turbine operated at 2000 rpm providing a high liquid flow, allowing a strong de-agglomeration of the precitates. The colloidal dispersions obtained were concentrated at 40–50°C maintaining a slight agitation, and then deposited in glass cm x 0.2 beakers and dried at 60°C for 48 h. Green monoliths ($1\times1\times0.2$ cm average size) were calcined at 500°C for 2 h, 1°C/min heating rate, and then sintered at temperatures up to 1500°C for 5 h with a heating rate of 2°C/min.

Powder morphology was observed by Transmission Electron Microscopy (TEM, Jeol 2000 FX). Adsorption–desorption isotherm curves and pore size distributions of unseeded and 10 wt% seeded Y-TZP powders were obtained by nitrogen adsorption at 77 K (Accusorb 2100, Micromeritics, USA).

Pore size distributions in green and calcined compact monoliths were obtained using mercury porosimetry (Autopore II, 9215). Sintered densities were measured by the Archimedes method with distilled water. Microstructure development was observed by SEM on both polished and fractured thermally etched surfaces and by TEM.

3. Results and discussion

3.1. Calcined powder characterisation

For the morphology analysis of Y-TZP powders, dried monoliths were ground, calcined at 350°C for 5 h, attrition milled for 2 h in pure 2-propanol with zirconia ball media, and dried at 80°C overnight. Typical TEM micrographs of the calcined powders are shown in Fig. 1. It can be noted from Fig. 1(a) that the morphology of the 10% seeded Y-TZP powder consisted of relatively agglomerated rounded crystallites with a uniform size distribution and sizes between 10 and 20 nm. Because of the low calcination temperature point contacts were the predominant bonding between particles. By contrast, Fig. 1(b) shows the poorly developed tetragonal zirconia particles from the unseeded air-calcined sample under the same experimental conditions. In this case, temperatures of 500°C are required for total crystallisation and, as a first consequence of this higher temperature, interparticle bonds appear, which detrimentally

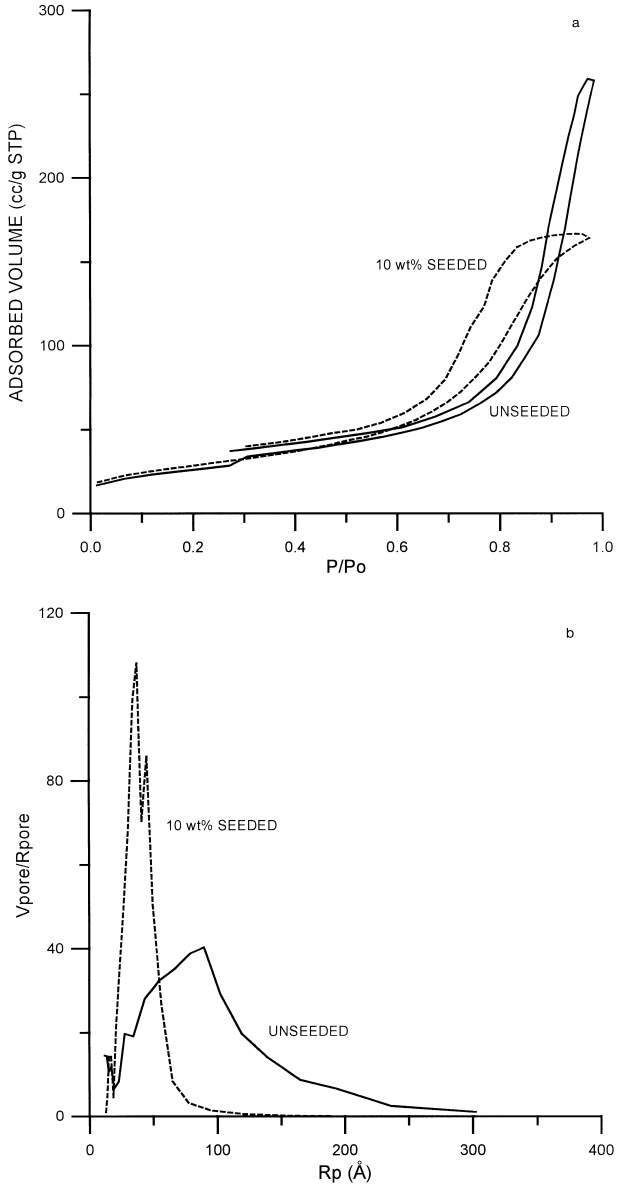

Fig. 2. Adsorption-desorption isotherm curves (a) and pore size distributions (b) for 10 wt% seeded and unseeded Y-TZP powders calcined at 500°C.

influence the compaction capability and the sinterability of Y-TZP crystallised powders.

The reasons for this reduced crystallisation temperature for seeded Y-TZP powders, is explained in previous works.[6,7] Basically the seeding of Y-TZP amorphous precursor with crystalline Y-TZP induced a nucleation and epitaxial growth process of the newly crystallised phase, which enhanced the crystallisation kinetics, and the activation energy is reasonably lowered.

Fig. 2(a) shows the adsorption–desorption isotherm curves, corresponding to type IV according to IUPAC nomenclature and are characteristic of mesoporous solids, The hysteresis loop corresponds to type A, for seeded powders and, type B for unseeded.[13] The pore size distributions of unseeded and 10 wt% seeded Y-TZP at 500°C are shown in Fig. 2(b). Both samples are mesoporous (as the isotherms indicate) but there is an important difference. While the seeded sample has a narrow pore size distribution (10–60 Å) the unseeded sample presents a wider range, almost 10 and 200 Å and the maximum located at about 90 Å. Such pore size distributions are a consequence of the agglomeration state of both Y-TZP powders.

3.2. Sintering behaviour of monoliths

Fig. 3 shows the pore size distributions in monoliths calcined at 500°C. While the average pore size diameter for green monoliths were of 17 and 15 nm for unseeded and seeded respectively, and therefore the compaction degree of both did not show significance differences, by contrast the average pore size diameter for these calcined monoliths were 20 and 7.5 nm for the unseeded and seeded, respectively. Not only has the seeded sample a lower average pore diameter but its pore size distribution is narrower (20–3 mn) than that of the unseeded. This last one has a wider pore size distribution with pore sizes between 5 nm and 1 μm in diameter, and although the presence of a second peak in the pore size distribution curve is not clear, a shoulder towards the smaller pore sizes is detectable, indicating a certain agglomeration degree in the unseeded green monoliths. This significant difference in the pore size is a consequence of the increased nucleation frequency for the crystallisation process. As a result of this a well-developed porous microstructure is obtained for these samples previous to the sintering. Similar results have been reported,[14,15] for obtaining of α-Al_2O_3 from boehmite gels seeded with α-Fe_2O_3. After transformation

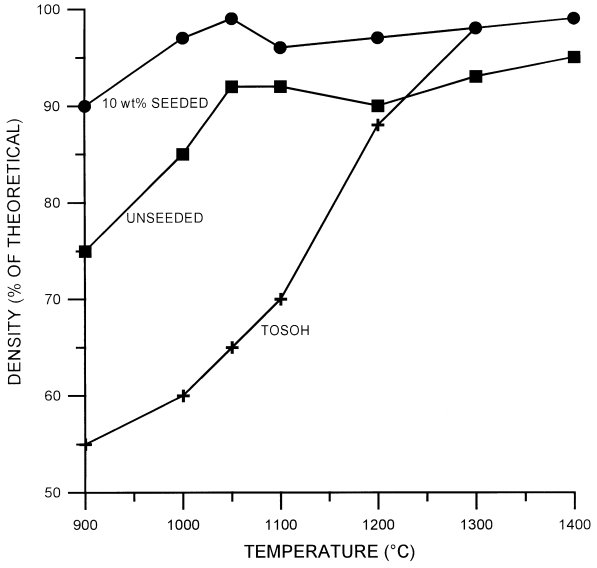

Fig. 4. Sintering behaviour as a function of the temperature of 10 wt% seeded, unseeded Y-TZP monoliths and commercial one

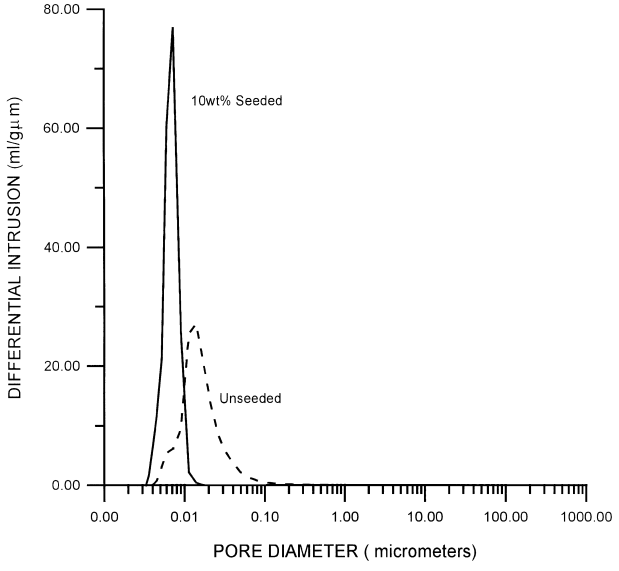

Fig. 3. Pore size distributions in 10 wt% seeded and unseeded Y-TZP monoliths calcined at 500°C.

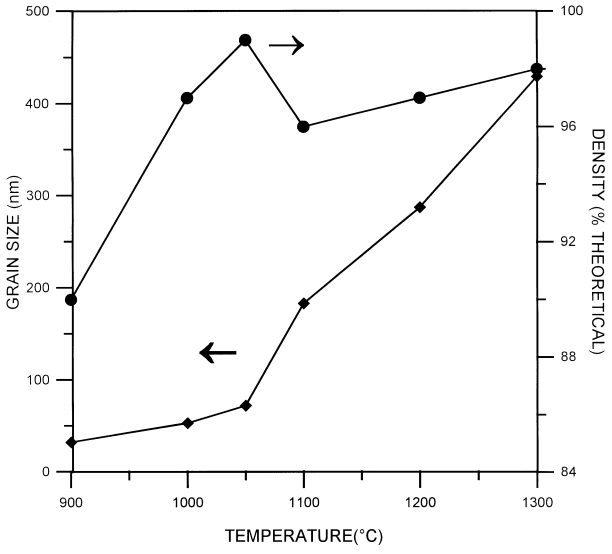

Fig. 5. Grain growth process in 10 wt% seeded sintered monoliths as a function of the sintering density and temperature.

to α-Al_2O_3, in unseeded gels, the pore radius increased by an order of magnitude and the pore size distribution is wider than seeded gels. Seeded samples developed a dense microstructure with a uniform grain structure at 1300°C, by contrast the unseeded showed the characteristic vermicular grain structure of α-Al_2O_3. Therefore, it could be predicted that the improved pore size distribution will strongly affect the sintering process, and the densification during sintering will proceed at lower temperatures and with higher rates in the case of the seeded Y-TZP monoliths.

Sintering behaviour as a function of the temperature of unseeded and 10 wt% seeded monoliths, previously heated at 500°C and a commercial one (Tosoh), was studied and is shown in Fig. 4. The samples were held at each temperature for 5 h with 2°C/min heating and cooling rates. In the case of the seeded samples a markedly enhanced sintering was observed during the early stages of sintering (below 1000°C). At 900°C the density was as high as 90% of the theoretical. At 1050°C the samples reached near theoretical density (≈99%), but between 1100 and 1200°C an abnormal sintering behaviour was observed and low densities (96%) were achieved. Above 1200°C and up to 1400°C again a high density (≈99%) was achieved. Although several causes can contribute to such abnormal densification,[16] the small particle size in the calcined seeded monoliths accelerated the densification kinetics at the early sintering stages leading to almost fully dense bodies at low temperature, see Fig. 5. For commercial samples,

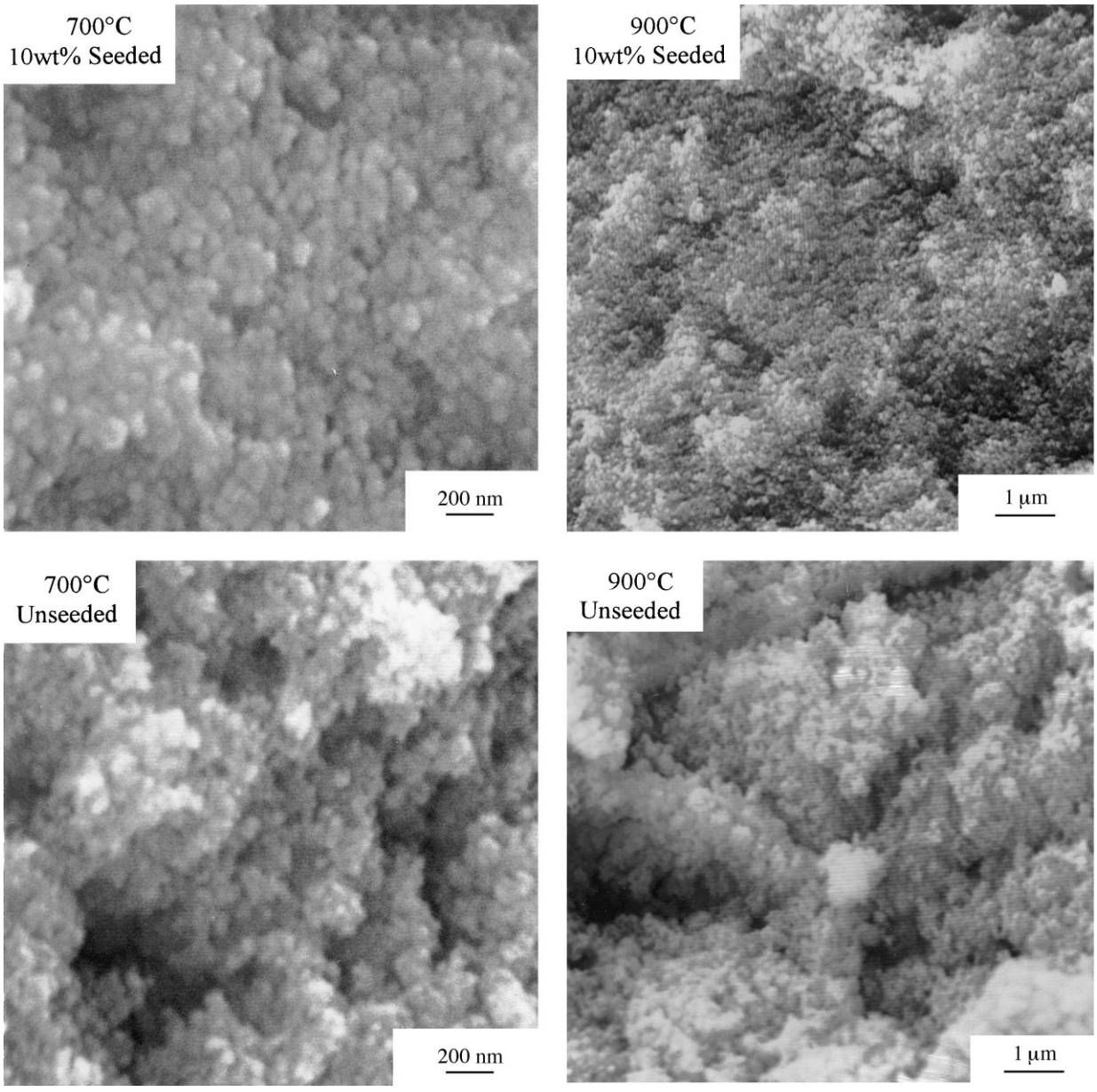

Fig. 6. SEM micrographs of the microstructure of fracture surfaces in Y-TZP monoliths 10 wt% seeded and unseeded, sintered at 700 and 900°C.

density monotonically increases with increasing temperature reaching near full density (>99%) at about 1300°C (250°C higher than for the seeded one). No abnormal densification was detected for the Tosoh samples. The presence of large agglomerates with relatively small pores but with a uniform pore size distribution in the green compacts, displaces the achievement of full density at higher temperatures.

Unseeded Y-TZP samples show, first, a rapid sintering with a maximum density between 1050 and 1100°C (92%), above and up to 1300°C lower densities, and then density increases with higher temperatures.

Although the densification curve aspect is very similar to the seeded one, much lower densities are obtained for unseeded ones. Clearly, as was described before, this is partially a consequence of the different pore size distribution of the calcined monoliths. Wider pore size distribution and higher pore size is detrimental to the densification process, and higher temperatures are required for complete densification.

Although grain size development also plays an important role on the sintering, the apparently abnormal sintering behaviour of these samples above 1050°C for seeded and unseeded samples could be interpreted, taking into account the critical pore-size to grain-size ratio postulated by Kingery et al.[16] The densification behaviour up to 1050°C could be justified because the majority of the pores are very small with respect to the grain size and, therefore, the pore-size to grain-size ratio is below the above postulated critical one. Above 1050°C and up to 1100°C a substantial grain size increase occurs, therefore, a certain pore coalescence takes place and the pore size to grain size ratio is higher than the critical one, then the density decreases, see Fig. 5. Above 1100°C a strong grain growth takes place, then the pore size to grain size ratio is below the critical ratio, the pores shrink and the density increases.

Fig. 6 shows the microstructure of fracture surfaces in Y-TZP monoliths. The micrographs corresponding to seeded samples sintered at 700 and 900°C show that the morphology and pore size are homogeneous and the grain size remain very small (well below 100 nm) and de-agglomerated. By contrast unseeded samples at these same temperatures exhibit a higher state of agglomeration and high level of interconnected porosity separating regions with more homogeneous grain morphology. These areas of porosity could act as a barrier for densification. In the case of α-Al_2O_3 obtained from boehmite and seeded with α-Fe_2O_3, McArdle and Messing[17] explain the effect of addition of these crystallographic suitable particles. These ones increase the nucleation frequency and the volume of material transformed per individual nucleation event is reduced, then the fraction of grain boundary area increases, enhancing the densification process. By contrast if the nucleation frequency is reduced the volume of material transformed is large per nucleation event, considering the shrinkage that takes place during the transformation, a high fraction of porosity remains after transformation around this large transformation area. The addition of seeds basically enhances and reduces the distribution of porosity, increasing the grain boundary fraction and facilitating the elimination of this porosity, controlling the grain size. As a result of all of this, lower temperatures are required for densification for seeded samples. In addition the enhanced kinetics of sintering reduced the thermal driving force responsible for grain coarsening during densification.

Fig. 7 shows the surface of seeded samples sintered at 1050°C–1200°C for 5 h. A grain size around 80 nm was measured at 1050°C. The fact that Y-TZP fully dense ceramics have been obtained at so low temperatures (1050°C) with a grain size within the nanometer range make it an interesting material for superplastic forming applications. In the case of the sintered unseeded samples the grain size, not shown here, was greater than 100 nm.

4. Conclusions

Yttria-doped tetragonal zirconia (Y-TZP, 3 mol% Y_2O_3) gel monoliths seeded with 10 wt% nanocrystalline Y-TZP particles, have been prepared by the coprecipitation of Zr^{4+} and Y^{3+} hydroxides and the stabilisation of the suspension. The presence of the seeding particles led to the formation of a homogeneous mesoporous microstructure in the monoliths with a narrow pore size distribution and a pore size as small as 7.5 nm. Such monoliths characteristics resulted in achieving near theoretically dense Y-TZP bodies at a temperature as low as 1050°C with a grain size within the nanoscale (<100 nm). An unseeded Y-TZP sample prepared under the same conditions was taken as a reference.

Acknowledgements

J. Tartaj thanks CSIC and The British Royal Society for the grant received for the development of part of this work.

References

1. Chen, D. J. and Mayo, M. J., Densification and grain growth of ultrafine 3 mol% Y_2O_3-ZrO_2 ceramics. *Nanostructured Mater.*, 1993, **2**, 469–478.
2. Durán, P., Recio, P., Jurado, J. R., Pascual, C. and Moure, C., Preparation sintering, and properties of translucent erbia-doped tetragonal zirconia. *J. Am. Ceram. Soc.*, 1989, **72**, 2088–2093.
3. Tani, E., Yoshimura, M. and Somiya, S., Formation of ultrafine tetragonal zirconia powders under hydrothermal conditions. *J. Am. Ceram. Soc.*, 1983, **66**(1), 11–14.
4. Boutz, M. M. R., Olde Scholtenhuis, R. J. M., Winnubst, A. J. A. and Burggraaf, A. J., A hydrothermal route for production of dense, nanostructured Y-TZP. *Mater. Res. Bull.*, 1994, **29**, 31–40.
5. Skandan, G., Hahn, H., Rooddy, M. and Cannon, W. R., Ultrafine grained dense monoclinic and tetragonal zirconia. *J. Am. Cerwn. Soc.*, 1994, **77**, 1706–1710.
6. Tartaj, J., Fernández, J. F., Moure, C. and Durán, P., Influence of seeding on the crystallisation kinetics of air-calcined Y-TZP gel-derived precursors. *Mat. Res. Bull.*, 1997, **32**, 1525–1533.
7. Tartaj, J., Fernández, J. F., Moure, C. and Durán, R., Effects of seeding on the crystallisation kinetics of

air-calcined yttria-doped hydrous zirconia. *J. Euro. Ceram. Soc.*, 1998, **18**, 229–235.
8. Kumagai, M. and Messing, G. L., Controlled transformation and sintering of a boehmite sol–gel by α-alumina seeding. *J. Am. Ceram. Soc.*, 1985, **68**, 500–505.
9. Suwa, Y., Roy, R. and Komameni, R., Lowering the sintering temperature and enhancing densification by epitaxy in structurally diphasic Al_2O_3 and Al_2O_3–MgO xerogels. *Mater. Sci. Eng.*, 1986, **83**, 151–159.
10. Durán, P., Tartaj, J., Femández, J. F., Villegas, M. and Moure, C., Crystallisation and sintering behaviour of nanocrystalline Y-TZP powders obtained by seeding-assisted chemical coprecipitation. *Ceramics Int.*, 1999, **25**, 125–135.
11. Klug, K. P. and Alexander, L. E., Crystallite size and lattice strains from line broadening. In *X-ray Diffraction Procedures*. John Wiley and Sons, New York, 1974, Chapter 9, pp. 618–708.
12. Mercera, P. D. L., Van Ommen, J. G., Doesbrug, E. B. M., Burggraaf, A. J. and Ross, J. R. H., Influence of ethanol washing of the hydrous precursor on the textural and structural properties of zirconia. *J. Mater. Sci.*, 1992, **27**, 4890–4898.
13. Gregg, S. J. and Sing, K. S. W., *Adsorption, Surface Area and Porosity*, 2nd edn. Academic Press, London, 1982, pp. 3–4, 116–117.
14. McArdle, J. L. and Messing, G. L., Transformation microstructure development and densification in α-Fe_2O_3-seeded boehmite-derived alumina. *J. Am. Ceram. Soc.*, 1993, **76**(1), 214–222.
15. Tartaj, J. and Messing, G. L., Anisotropic grain growth in α-Fe_2O_3-doped alumina. *J. Euro. Ceram. Soc.*, 1997, **17**, 719–725.
16. Kingery, W. D., Bowen, H. K. and Uhlmann, D. R., *Introduction to Ceramics*, 2nd edn. John Wiley and Sons, New York, 1976, pp. 486.
17. McArdle, J. L. and Messing, G. L., Transformation and microstructure control in boehmite-derived alumina by ferric oxide seeding. *Adv. Ceram. Mater.*, 1988, **3**(4), 287–392.